Confirmation of 3D basin structure models by long-period ground motion simulation – in case of Osaka basin, western Japan

Asako Iwaki and Tomotaka Iwata (DPRI, Kyoto University, JAPAN)

e-mail: iwaki@egmdpri01.dpri.kyoto-u.ac.jp

Introduction

Osaka area, one of the most populated areas in western Japan, is located inside a sedimentary basin whose size is approximately 60km x 40km with bedrock depth of 3km at the deepest. Because of this kind of underground structure, long-period ground motions with large-amplitude and long-duration are expected during huge size earthquakes. In fact, long-period ground motions were observed at strong motion stations inside Osaka basin during the 2004 Off Kii peninsula earthquake sequence (M_{JMA}5-7). In this study, we conducted ground motion simulations using two kinds of 3D basin structure models and evaluated the applicability of the models for the long period ground motion simulations by comparing observed and simulated ground motions.

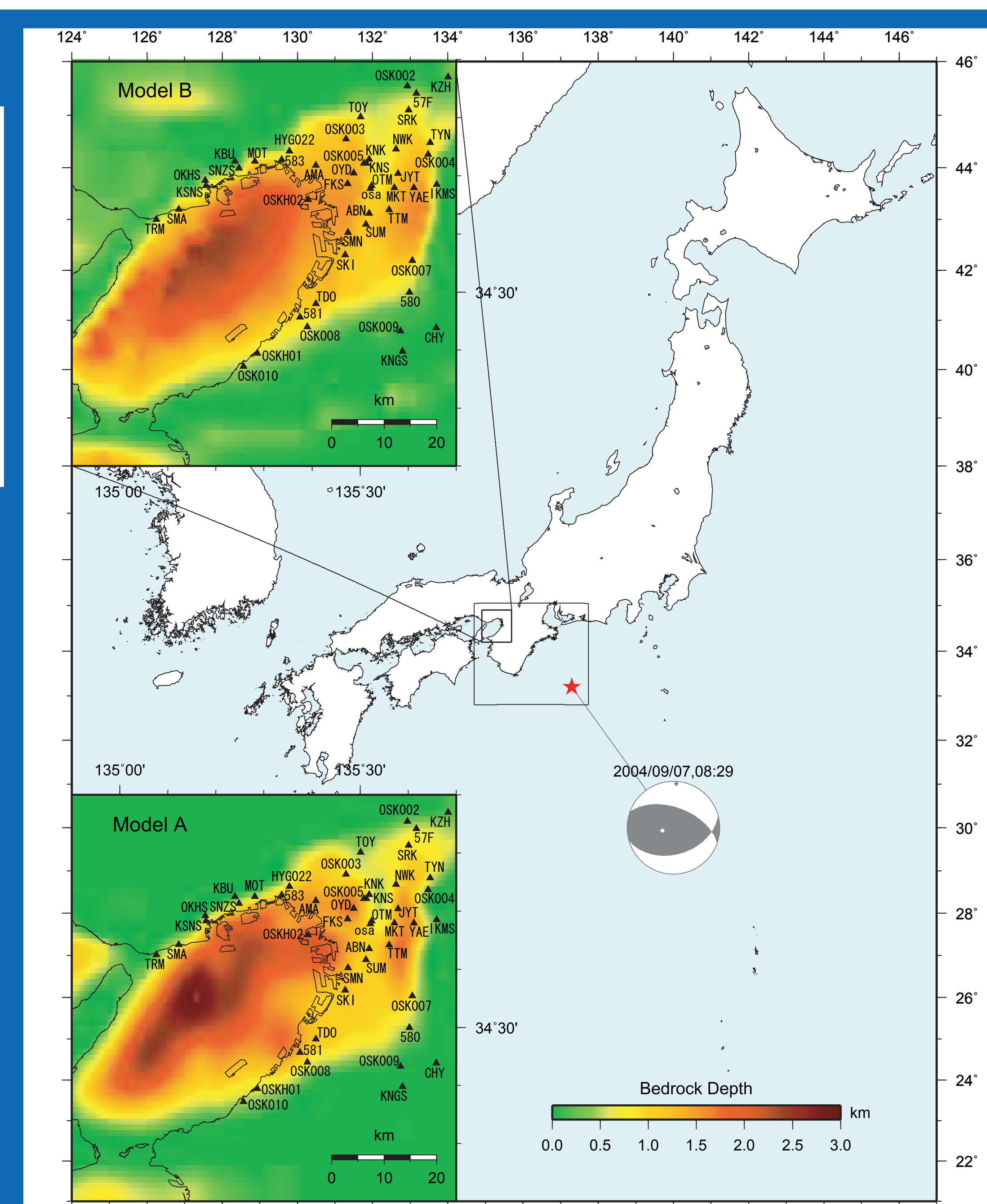

Figure 1. Map of study area, including area of calculation (large rectangle), Osaka basin area (small square), and the epicenter of 2004/09/07 M6.5 earthquake. Bedrock depth of the basin structure models together with strong motion stations used in this study are also shown (left bottom: Model A, left top: Model B).

Ground motion simulation

We conducted ground motion simulations of the largest aftershock of the 2004 Off Kii peninsula earthquake (2004/09/07 08:29JST, M_{JMA}6.5) by 3D finite-difference method (Pitarka, 1999). The velocity structure model comprises two parts: inside the basin (3D) and outside the basin (1D). Using this model we generated the waveform of a basin site i by defining a transfer function

$$T_i(\omega)=P_i(\omega)/P_r(\omega)$$

as the relation between waveforms of a basin site i and the reference site r (CHY in this study). Thus the synthetic waveform at basin station i is

$$S_i(t)=T_i(t)*obs_r(t)$$

where $obs_r(t)$ is the observed record at CHY.

Table 1. Velocity structure models

Model A (Kagawa et al., 2004)

	Vp (km/s)	Vs (km/s)	ρ (g/cm^3)	depth (km)
1	1.60	0.35	1.7	0.193h
2	1.80	0.55	1.8	0.472h
3	2.50	1.00	2.1	h
1	5.40	3.20	2.7	3.1
2	6.00	3.70	2.8	15
3	6.70	3.90	2.9	35
4	7.70	4.45	3.1	50

Model B (Horikawa et al., 2003)

	Vp (km/s)	Vs (km/s)	ρ (g/cm^3)	depth (km)
1	1.53	0.30	1.65	variable
2	1.64	0.40	1.78	
3	1.76	0.50	1.87	
…				
17	4.20	1.90	2.50	
1	5.50	2.75	2.6	3.0
2	6.00	3.70	2.8	15
3	6.70	3.90	2.9	35
4	7.70	4.45	3.1	50

Model size : 260km x 290km x 50km
Basin area : 90km x 90km x 3km
Minimum grid : 0.125km (inside the basin), 1km (outside the basin)
Frequency range of calculation : up to 0.33 Hz

Table 2. Source model parameters (point source)

Latitude	Longitude	Depth	Strike	Dip	Slip	Source duration	M_0	M_W
N33.209°	E137.293°	25km	272°	49°	97°	3.0sec	6×10^{18}Nm	6.5

Simulation results

Transfer function

We investigated spatial distribution of theoretical transfer function $T(\omega)$ (period 3-20s) inside the basin in terms of amplitude and peak period. Both implied significant influence of the basin structure upon the wave propagation inside the basin. Amplification compared to the reference rock site (CHY) reached nearly 30 at period 3-8s.

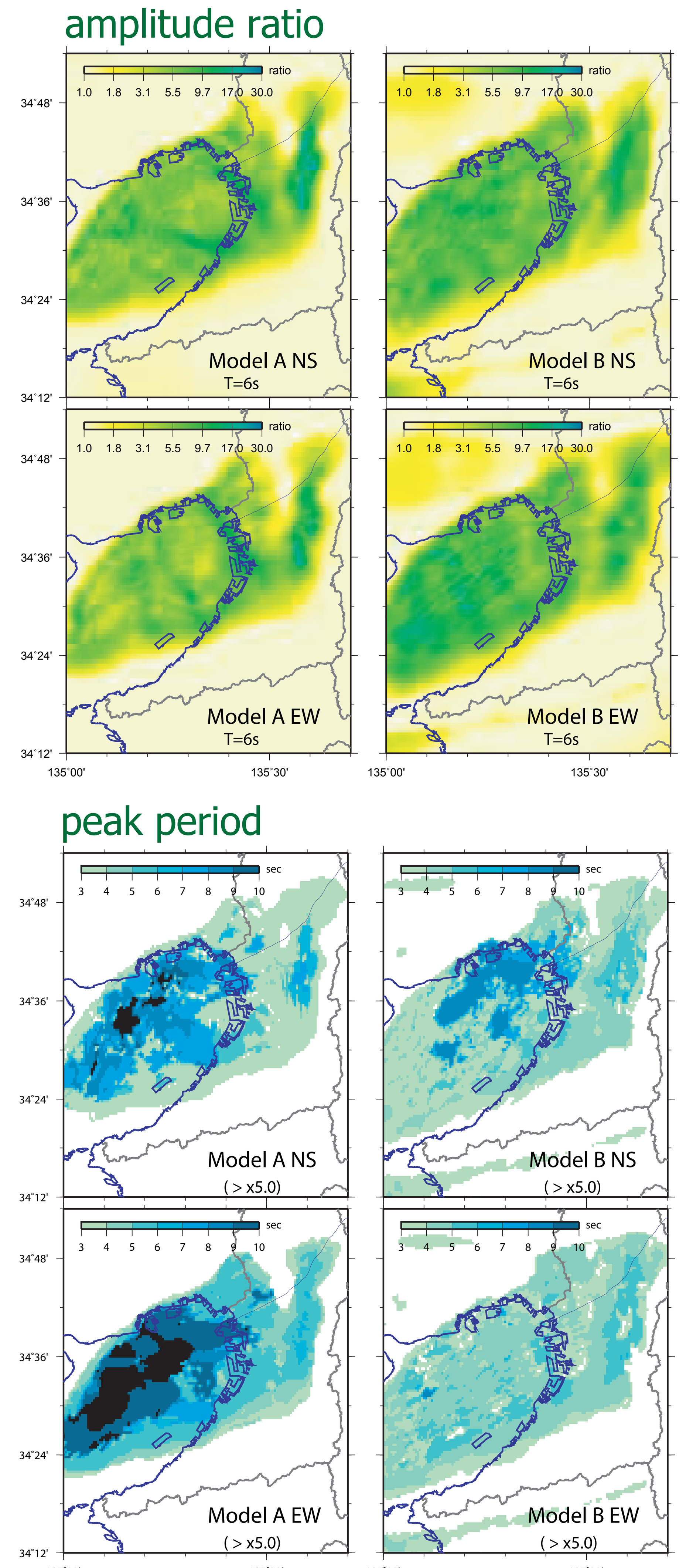

Figure 2. [Top panel] Transfer function amplitude (period=6s) for Model A (left) and Model B(right). [Bottom panel] Peak period t_p of transfer function. Plotted only if the peak amplitudes at t_p are more than 5.

Waveforms

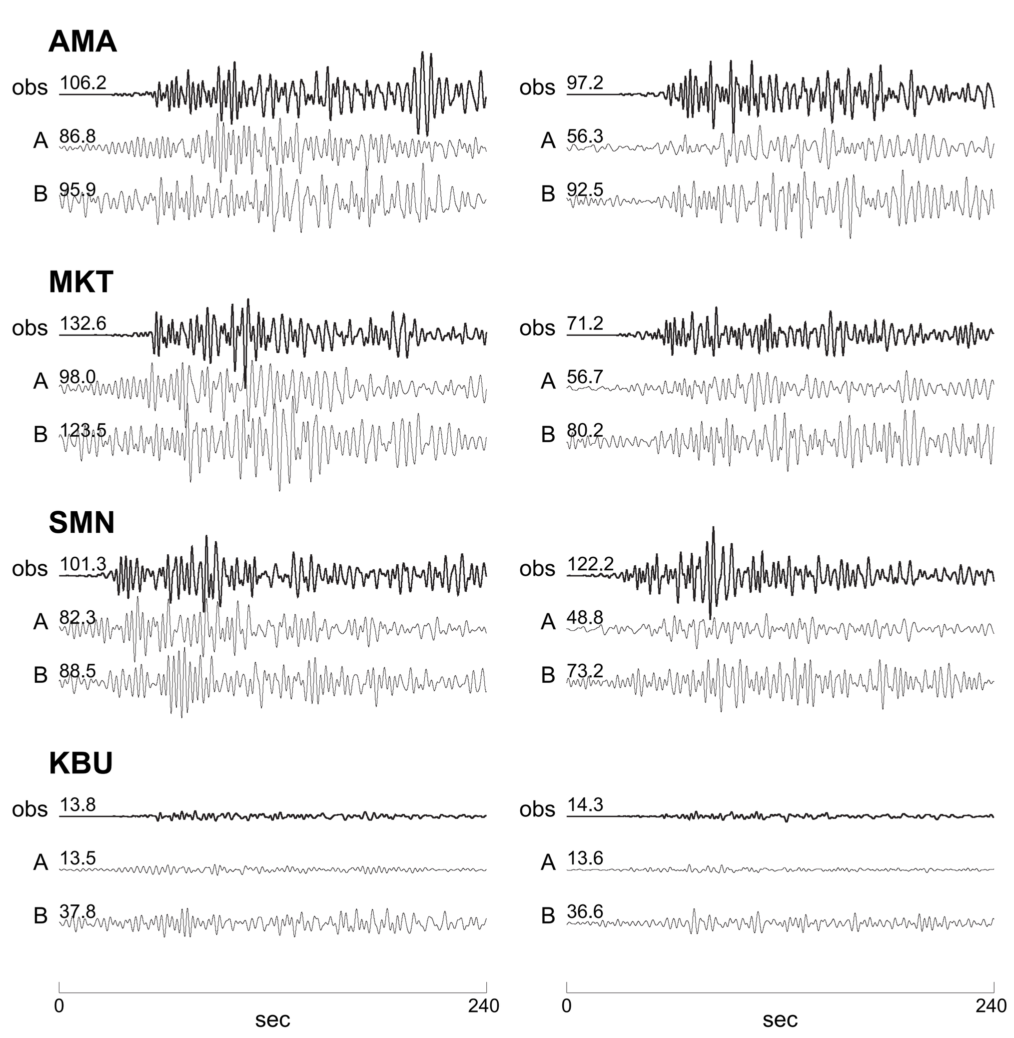

Figure 3. Examples of waveforms of 2 horizontal components (left: NS, right: EW) compared with observed veolocity records (filtered 3-20s).
[AMA and MKT] Waveforms are well reproduced for both Model A and Model B.
[SMN] EW component is underestimated for Model A.
[KBU] Both components are overestimated for Model B.

Pseudo velocity response spectra

Psuedo velocity responce spectra (h=5%) was calculated from synthetic and observed waveforms for period between 3-20s. Both models well reproduced the observed response spectra at most stations, especially near the predominant periods. However, there are some stations where either/both model(s) did not well reproduce the amplitudes or predominant periods.

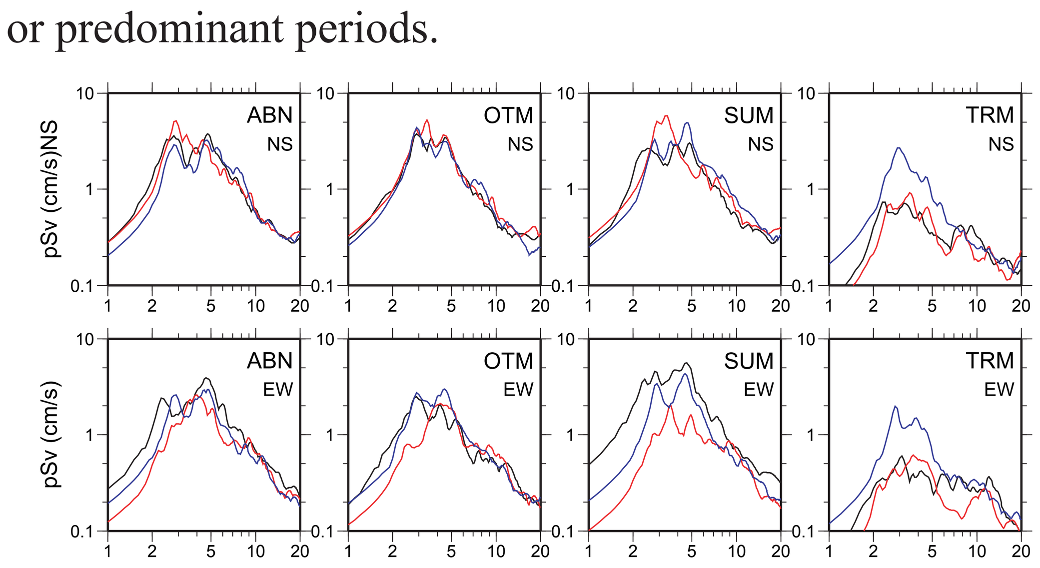

Figure 4. Examples of pSv (h=5%) of observation (black line), Model A (red line), and Model B (blue line).
[ABN and OTM] Well reproduced for both models.
[SUM] EW component is underestimated for Model A.
[TRM] Overestimated for Model B.

Goodness of fit of pSv

We estimated the goodness of fit between simulated and observed pSv (3-20s) using the following factor (Pitarka *et al.*, 2004).

$$f=2\frac{\int p(T)_{obs}\,p(T)_{syn}dT}{\int (p(T)_{obs}^2+p(T)_{syn}^2)dT} \qquad p(T):\ \text{pSv}$$

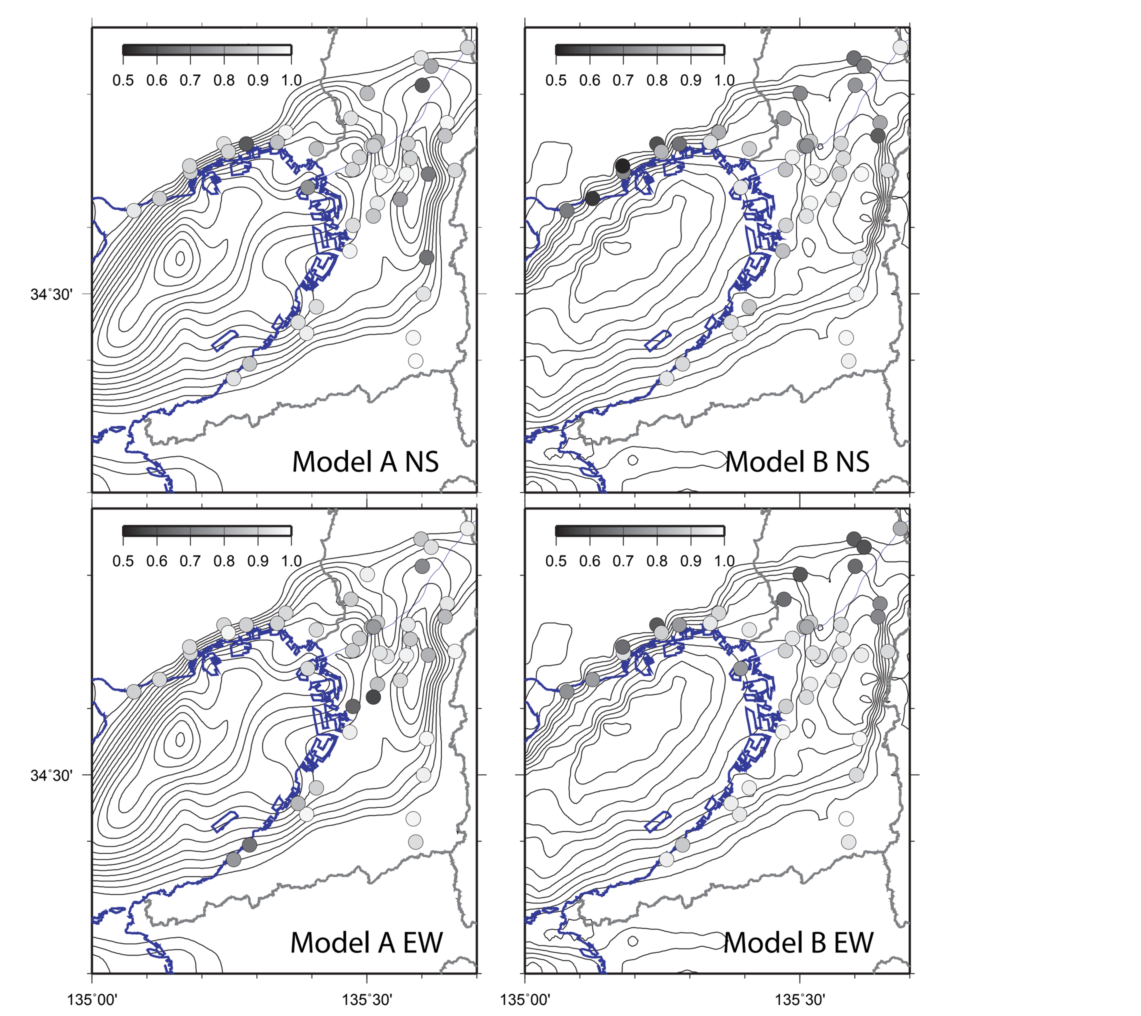

Figure 5. Goodness-of-fit factor f for pSv (period 3-20s). Syn. and obs. match each other perfectly when f=1. Contour lines indicate the distribution of bedrock depth of each model.

Conclusions

We conducted long-period ground motion simulations using velocity structure models that contain 2 types of 3D Osaka basin structure models and a 1D structure model. We introduced the transfer function method that employ observed record at a reference site. In order to evaluate the applicability of the Osaka basin velocity structure models for long-period ground motion, we compared the simulation results with observed records. Both basin structure models reproduced fairly well in terms of waveforms and pSv. However, at some stations simulations did not reproduce the observation well enough, especially where the bedrock depth sharply changes. In specific, for Model A, synthetic ground motions of EW-component were less estimated at stations located in southern Osaka, such as SMN and SUM, and pSv showed notable misfit at stations near eastern edge of Osaka basin, such as SRK, YAE, OSK007 and 583. For Model B, synthetic waveforms and pSvs did not agree well at stations located in Kobe area and northern Osaka, such as MOT, KBU, TRM, SMA, SRK and OSK002.